Synthesis and Luminescent Characteristics of $(Ca_{4-x-y-z}Ba_ySr_z)(PO_4)_2O:xEu^{2+}$ Phosphors as a Potential Application for White-Light Emitting Diode

G. Deressa

School of Applied Natural Science, Department of Applied Chemistry, Adama Science and Technology University, Adama 1888, Ethiopia Email:

Abstract

A novel tunable red- to yellow- emitting phosphor,$(Ca_{4-x-y-z}Ba_ySr_z)(PO_4)_2O:xEu^{2+}$ is reported that displays a broad emission from 500 to 800nm, and its emission can be adjusted from red to yellow by changing Ba^{2+} and Sr^{2+} doping concentration. X-ray powder diffraction analysis confirmed the phase formation. Excitation and emission spectra, and concentration dependence of emission intensity of the phosphor were investigated. The results showed that with increasing Ba^{2+}/Sr^{2+} concentration, the emission peak wavelength blue-shift from 594 to 567 nm, and the color can be tuned from red to yellow. When single- phase $(Ca_{2.95}Ba_{0.5}Sr_{0.5})(PO_4)_2O:0.05Eu^{2+}$ phosphor is pumped by a blue InGaN light-emitting diode we obtain white light with color rending index between 80.0 and 88.0 and color temperatures between 3500 and 5450 K, suggesting that this material is competitive as a color conversion material for solid state lighting.

Keywords*: White light-emitting diode; Phosphors; Tunable emitting*

1. Introduction

The commercialized white light emitting diodes (WLEDs) can be generated by combining a blue-emitting InGaN-LED chip and a yellow-emitting garnet phosphor $Y_3Al_5O_{12}:Ce^{3+}(YAG:Ce^{3+})$ (Bachmann *et al*., 2009; Schubert *et al*., 2005 and Deressa *et al*., 2015). However, such white light does not have sufficient color rendering properties. The color-rendering index (CRI) remains to be improved due to the lack of a full color component from the yellow phosphor. Recently, several WLED devices fabricated using ultraviolet (UV) chip coupled with a blend of tunable (blue-to-yellow) emitting and red-emitting phosphor, which exhibited favorable properties,

34

including tunable correlated color temperature (CCT), tunable Commission International del' Eclairage (CIE) chromaticity coordinates, and excellent CRI values (Deressa *et al.*, 2015; Setlur *et al*., 2010; and Zhou *et al*., 2014).Unfortunately, the emission tunable range of the phosphor with a single activated ion has been reported is limited to blue to yellow.

Changing the cation ratio of orthophosphate phosphate can distort the lattices structure due to change in crystal field of the host that causes the broadening spectra of the luminescence.This is also a promising host for lighting and display due to its good thermal stability and high luminescent efficiencies. The Eu^{2+}-activated OrthophosphatePhosphates are good candidates as host structures and offer a number of merits, such as high chemical and low synthesis temperature and physical stability, and they exhibit interesting

luminescence (Yang *et al*., 2004; Zhou *et al*., 2013).

The motivation of this work was to invesigate a tunable red to yellow-emitting and efficient inorganic phosphors $(Ca_{4-x-y-z}Ba_ySr_z)(PO_4)_2O:xEu^{2+})$ that could be applied in UV or blue LEDbased solid state white light sources.

Orthophosphate-phosphor doped with rare earth ions is widely explored as red, green and blue (RGB) phosphors owing to advantages of relatively low sintering temperature, good chemical stability, and satisfactory absorption in the ultraviolent (UV) to blue region (Zhou *et al.*, 2013; Huang *et al*., 2008). $Ca_4(PO_4)_2O:Eu^{2+}$ is novel red-emitting phosphate phosphors (Kottaisamy *et al*., 1994). To the best of our knowledge, its tunable emitting properties have not been reported in the literature. In this paper, we investigated a tunable red- to yellow- emitting $(Ca_{4-x-y-z}Ba_ySr_z)$

35

$(PO_4)_2O:xEu^{2+}$ phosphor. This phosphor was excited by light in UV to blue region and showed tunable red-to-yellow emission. The optical properties of Orthophosphate phosphate phosphors were systematically investigated by means of photoluminescence excitation (PLE) and emission (PL) spectra, thermal stability, Raman, and applications for white light emitting diodes (white-LEDs).

2. Materials and Methods

2.1. Preparation $(Ca_{4-x-y-z}Ba_ySr_z)$ $(PO_4)_2O:xEu^{2+}$ phosphate phosphors

Powder samples of Orthophosphate phosphors were prepared by a solid-state reaction. MCO_3 (99.99%), [M = Ca, Sr and Ba], $(NH_4)_2HPO_4$ (99.0%), and Eu_2O_3 (99.99%) are weighed, thoroughly mixing and ground in an agate mortar. The mixed powders were then transferred into an alumina crucible, and pre-sintered in a furnace at 500 °C for 2 hours in air to eliminate the water and decompose the carbonate. The pre-sintered samples were subsequently cooled down to room temperature and fully ground to form a homogeneous mixture. Then the mixture was re-sintered at a high temperature of 1000 to 1300 °C for 4 hours under a reducing atmosphere (5%H_2/95%N_2) for 4 hours. After sintering, the samples were cooled down naturally to room temperature in the furnace. The acquired sintered products were pulverized for further measurements. The nominal molar compositions of the phosphors are: $Ca_{4-x-y}Ba_ySr_z(PO_4)_2O:_xEu^{2+}$ (0.01 ≤ X ≤ 0.10, 0 ≤ Y ≤ 2.5, and 0 ≤ Z ≤ 2.5)) (Setlur *et al.*, 2010)

2.2. Materials Characterization

The as-prepared samples were characterized by using the following instruments; Scanning electron microscope (SEM: LEO SUPRA 55, Carl Zeiss) attached

with an energy dispersive X-ray spectrometer (EDX), X-ray diffractometer (M18XHF - SRA, Mac Science), X-ray diffraction (XRD) analysis using a Rigaku D/MAX 2500 with Cu Kα radiation. The measurements of photoluminescence (PL) and photoluminescence excitation (PLE) spectra are carried out using a DARSA PRO-5200 fluorescence spectrophotometer equipped with a xenon lamp as the excitation light source. The thermal quenching characteristics are measured in the temperature range of 25-200 °C. Raman spectra of $(Ca, Sr, Ba)_4(PO_4)_2O$: Eu^{2+} were carried out at room temperature in the range of 200 to 2000 cm^{-1} using Agiltron, Raman Spectrometer, which is having excitation Nd:YAG laser) a excitation laser source (1064 nm).

2.4. LED Lamp Fabrication.

The WLEDs were fabricated using a blue-LED chip with a 450 nm excitation wavelength. First of all, the chip was assembled on a LED frame and care was taken to prevent the formation of air bubbles between the chip and frame, because it can damage the LED when a forward bias current is applied. The semi-transparent silicone epoxy was prepared by mixing two optical encapsulates, i.e., OE-6630 A (base) and OE-6630 B (catalyst) in 1:2 ratio. Afterwards, the required quantity of $(Ca_{2.95}Ba_{0.50}Sr_{0.50}Eu_{0.05})(PO_4)2O$ phosphor powders were mixed with the silicone epoxy, kept in a mixer and later kept in a desiccator to remove the air bubbles. Finally, it was poured in a dispenser tube. The phosphor mixed epoxy was later dispensed onto the LED frame and kept in an oven (@ 120 °C, for 90 min) to harden, and eventually the WLEDs were characterized by using an OL770 multi-channel spectroradiometer attached with an integrating sphere (Deressa et al., 2015).

3. Results and Discussion

3.1 Phosphor Synthesis and Characterization.

Fig.1 shows the results of the data collection and structure refinements for $(Ca_{2.95} Ba_{0.50} Sr_{0.50} Eu_{0.05}) (PO_4)2O$. The single crystal structure data of $Ca_4(PO_4)2O$ (ICSD no. 2631) was performed as starting reference to approach the actual crystal structure. The final converged weighted-profile of Rexp=6.99, Rwp= 9.16, Rp=7.09

and GOF=1.31 is shown in Table 1. The $(Ca_{2.95} Ba_{0.50} Sr_{0.50} Eu_{0.05})$ $(PO_4)2O$ crystallizes in a monoclinic unit cell with space group P21(4) space group with Z = 4. In the crystal structure of $Ca_4(PO_4)2O$, the Ca^{2+} ions have eight different coordination environments, only Ca(6) ion is eight-coordinated, and the other Ca^{2+} ions are seven-coordinated (See Fig. .1 (b)

Table 1: Rietveld refinement and crystal data of Rietveld enhancement and crystal data of $(Ca_{2.95}Ba_{0.50}Sr_{0.50}Eu_{0.05})(PO_4)2O$ phosphors

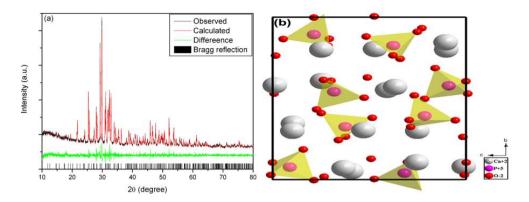| Formula	$Ca_{3.95}(PO_4)_2O:0.05Eu^{2+}$
Cryst. syst.	$P2_1(4)$ – monoclinic
Crystal Density (g/cm^3)	7.229
Units, Z	4
a (Å)	7.012 (11)
b (Å)	11.979 (13)
c (Å)	9.481 (9)
V (Å^3)	797.32576(15)
β (deg)	90.6(2)
R_{exp} (%)	6.89
R_{wp} (%)	9.14
R_p (%)	7.06
GOF	1.29

Figure1: (a) Observed (black), calculated (red), and difference (green) synchrotron XRD profiles for the Rietveld refinement of $(Ca_{2.85}Ba_{0.50}Sr_{0.50})(PO_4)_2O:0.05Eu^{2+}$. Bragg reflections are indicated with tick marks. (b) Crystal structure of $Ca_4(PO_4)_2O$ unit cell viewed in a-direction (Deng*et al.*, 2013).

The XRD patterns of $(Ca_{4-y-z}Ba_ySr_z)(PO_4)_2O:0.05Eu^{2+}$ together with the Joint Committee on Powder Diffraction Standards (JCPDS) card No. 73-1379 are shown in Fig. 2. When the Sr^{2+} doping content (z), the diffraction peaks of the obtained sample can be indexed to the standard data except for little shift, indicating that these samples almost are single-phase. When the Ba^{2+} doping content (y), the diffraction peaks of the obtained sample can be indexed to the standard data except for little shift, indicating

that these samples almost are single-phase. $Eu^{2+}/Ba^{2+}/Sr^{2+}$ are incorporated in the host lattice (Yang *et al.*, 2004).

When the Ba^{2+} doping content (*y*) is higher than 0.10, the intensity of some crystal planes diffraction peaks increased gradually, such as (200), (210) and (212) which indicated that with the increase of Ba^{2+} ions substiturion, resulted in corresponding crystal face preferred growth. Additionally, the diffraction peaks exhibited a shift toward smaller angles with rising doping content of the Ba^{2+} ion,

39

which may be related to the substitution of smaller Ca^{2+} by the lager Ba^{2+}. The micromorphology of the crystalline $(Ca_{2.95} Ba_{0.50} Sr_{0.50} Eu_{0.05}) (PO_4)_2O$ phosphor sample observed by SEM is shown in Fig. 3. It is observed that the particles have smooth morphology and the diameters are ranging from 15 to 20 μm. The elemental composition of $(Ca_{2.95} Ba_{0.50} Sr_{0.50} Eu_{0.05}) (PO_4)_2O$ sample verified by EDS shows (wt %) Ca 35.28%, Ba 3.23%, Sr 3.38, Eu 2.25 %, P 16.34 % and O 38.91%. The composition suggested by EDS is consistent with stoichiometric weight ratio with reasonable relative error.
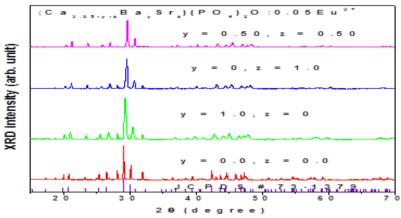

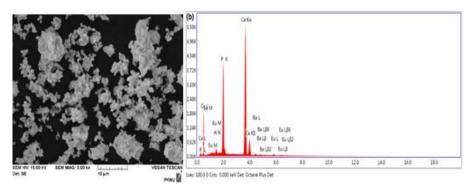**Figure 2:** XRD patterns of $(Ca_{4-y-z}Ba_ySr_z)(PO_4)_2O:0.05Eu^{2+}$ phosphors

Figure 3: (a) SEM image and (b) EDS profile of $(Ca_{2.95}Ba_{0.50} Sr_{0.50}Eu_{0.05})$ $(PO_4)_2O$ sample

The Raman vibrational frequencies of v_2, v_3, and v_4 are follows the same phenomenal. The shift in the observed Raman frequencies is believed to be due a tightening or enlargement of the molecular PO_4^{3-} ion as oxygen atoms of neighboring molecules are either drawn near or pushed apart on substitution of cations of different size. The bond length of Ba-O/ Sr-O are longer than the C-O in the crystal structure of Ba$_4$ PO)$_2$O,Sr$_4$PO$_4$)$_2$O and Ca$_4$PO$_4$)$_2$O, respectively. The crystal structure of (Ca$_{2.95}$Ba$_{0.50}$Sr$_{0.50}$) (PO$_4$)$_2$O:0.05Eu^{2+} formed from mixed crystal structure of Ba$_4$PO$_4$)$_2$O,Sr$_4$PO$_4$)$_2$O and Ca$_4$PO$_4$)$_2$O as observed from XRD and Raman properties of the structures, Both XRD and Raman spectra of the host (Ca$_{2.95}$Ba$_{0.50}$Sr$_{0.50}$) (PO$_4$)$_2$O found between these three hosts of Ba$_5$(PO$_4$)$_3$Cl and Sr$_5$(PO$_4$)$_3$Cl lattices. This indicate that the lattices of (Ca$_{2.95}$ Ba$_{0.50}$ Sr$_{0.50}$) (PO$_4$)$_2$O host combined from an expanded Ba-O/Sr-O and

contracted Ca-O bonds which create different environments around the sites of Eu^{2+} ions doped in the lattice of (Ca$_{2.95}$ Ba$_{0.50}$Sr$_{0.50}$)(PO$_4$)$_2$O phosphor and cause for the blue shifts and spectral broadening of Eu^{2+} activated (Ca$_{2.95}$ Ba$_{0.50}$ Sr$_{0.50}$) (PO$_4$)$_2$O phosphors (Setlur *et al.*, 2010; Im *et al.*, 2010).

The excitation and emission spectrum of (Ca$_{2.95}$ Ba$_{0.50}$ Sr$_{0.50}$) (PO$_4$)$_2$O:0.05Eu^{2+} are shown in Fig. 5. Under 450 nm excitation, there are the broad asymmetric emission spectrum peaking at 567 nm with four broad emission bands centered at 567, 608, 632 and 667 nm, respectively. The broad emission shows that Eu^{2+} has more than one emission center in Ca$_4$(PO$_4$)$_2$O which belongs to the typical emission of Eu^{2+} ions ascribed to 5d→4f transitions. By Gaussian deconvolution, the emission spectrum of (Ca$_{2.95}$ Ba$_{0.50}$ Sr$_{0.50}$)(PO$_4$)$_2$O:0.05Eu^{2+} can be well-decomposed into eight Gaussian proflies peaking at 534

41

nm, 556 nm, 567 nm, 592, 608 nm, 632 nm, 667 nm, 673 nm and 674nm, which can be ascribed to eight different Ca^{2+} sites occupied by Eu^{2+} ions. The refinement shows that the structure of $Ca_4(PO_4)_2O$ contains eight crystallographically distinct Ca^{2+} sites that can be occupied by Eu^{2+}. The Eu^{2+} ions substituting Ca^{2+} ions in the site which has shorter Ca-O band distance are expected to experience stronger crystal field strength corresponding to a longer wavelength emission with larger Stoke shift, when the crystal environments are analogous. Fig. 5illustrates eight kinds of cations

ions coordinated with oxygen atoms, corresponding to the eight Gaussian profiles in the emission spectrum (Schubert *et al*., 2005; Deressa *et al*., 2015 and Wu *et al*., 2011).

It is also observed that the excitation spectrum monitoring by 594 nm exhibits a different spectral profile, which means that the Ba/Sr substitute Ca at diferent site in the lattics and emission bands should be ascribed to different sites occupied by Eu^{2+} ions, which is also in accordance with the above analysis on the crystal structure.
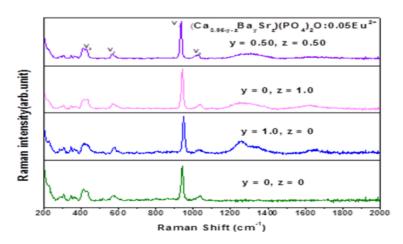

Figure 4. Raman Spectra of $(Ca_{4-y-z}Ba_ySr_z)(PO_4)_2O:0.05Eu^{2+}$ phosphor

42

The excitation spectrum shows a broad absorption from 300 to 500 nm with different maximum in the range, which corresponds to the $4f^7 \rightarrow 4f^6 5d^1$ transition of the Eu^{2+} ions. $(Ca_{3.95-y-z}Ba_y Sr_z)(PO_4)_2 O{:}0.05Eu^{2+}$ can be efficiently excited by blue light (350~480 nm), which is very advantageous for application in the W-LEDs combined with highly efficient blue-InGaN chips (Fig. 6b) (Zhou*et al*., 2014; Dorenbos*et al*., 2013 and Zhou *et al*., 2013).
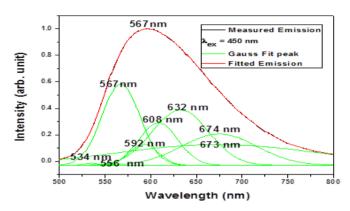

Figure 5: Emission spectra of $(Ca_{2.95}Ba_{0.50}Sr_{0.50})(PO_4)_2 O{:}0.05Eu^{2+}$ (λ_{ex} = 450nm) measured emission (black line), fitted curve (red line) and deconvoluted Gaussian curve

Fig. 6(a) shows room temperature normalized PL spectra of $(Ca_{3.95-y}Ba_y)(PO_4)_2 O{:}\ 0.05Eu^{2+}$ phosphors for an excitation wavelength of 450 nm. The emission intensity at 594nm shifted to shorter wavelength as Ba^{2+}/Sr^{2+} substituted in the lattices of Ca^{2+} ion. In general, the electronic configuration of Eu^{2+} is $4f^7$ and $4f^6 5d^1$ at the ground and excited state, respectively, and the luminescence of Eu^{2+} is ascribed to the $4f^6 5d^1$ into $4f^7 5d^0$ transition which results in the broad band emission. The emission wavelength of Eu^{2+} depends strongly on the structure of the host crystal through the crystal field splitting of the 5d band and the ground state for the
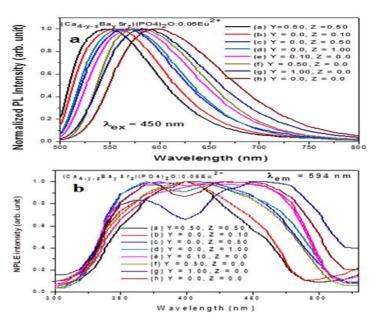
43

$4f^7$ electronic configuration (Zhou *et al*., 2013; Kottaisamy *et al*., 1994 and Huang *et al*., 2008).

Figure 6: (a) Emission spectra (λ_{ex}= 450nm) and, (b) Excitation (λ_{em}= 594) of ($Ca_{3.95-y-z}Ba_ySr_z$) $(PO_4)_2O$: $0.05Eu^{2+}$).

As stated above, the positions of the $4f^6d^1$ levels are much more influenced by the outer crystal field interaction than the $4f^7$ levels and highly depend on the crystalline environment around Eu^{2+} ion, so significant optical changes are expected if local structure around the Eu^{2+} center is different (Schubert *et al*., 2005; Deressa *et al*., 2015). In case of as-synthesized $Ca_{3.95-y-z}Ba_ySr_z)(PO_4)_2O$:$0.05Eu^{2+}$

phosphors, the environment around Eu^{2+} ions have uniform crystal structures. The unit cell volume of $Ca_4(PO_4)_2O$ is less than $Ba_4(PO_4)_2O$ and $Sr_4(PO_4)_2O$ hosts due to ionic size difference of Sr^{2+}/Ba^{2+} and Ca^{2+} ions and the ionic size of Eu^{2+} less than that of Sr^{2+} and Ba^{2+} ions, upon Eu^{2+} doping in to the above hosts. The is $Ba_4(PO_4)_2O$ and $Sr_4(PO_4)_2O$ less than slightly distortion than

44

$Ca_4(PO_4)_2O$ hosts because of the size difference between Eu^{2+} and Ba^{2+}/Sr^{2+} bigger than the size of Ca^{2+} ions. Therefore, PL spectrum of the dopant Eu^{2+} ion experienced strong crystal fields (blue shift) and low symmetry (broaden) in $Ca_{4-y-z}Ba_ySr_z)(PO_4)_2O$ than $Ca_4(PO_4)_2O:0.05Eu^{2+}$ phosphors, due to local structure (symmetry) difference around Eu^{2+} center in the respective hosts.

When content of Ba^{2+}/Sr^{2+} ions increased from ($y = 0.1$ to 1.0, and $z = 0.1$ to 1.0) the emission peak positions gradually move toward longer wavelengths from 549 nm to 594 nm, and in addition, the FWHM of Eu^{2+} ions emission broaden from 140 nm to 210 nm (see Fig. 6(a)). For $(Ca_{3.95-y}Ba_y)(PO_4)_2O:0.05Eu^{2+}$ phosphors, about 70 nm shift and 51 nm broadening allow highly color-tunable phosphors by changing the content of Ba^{2+}/Sr^{2+} ions (Ronda *et al*., 2008; Sommerdijk *et al*., 1974 and Wegh *et al*., 1999).

This indicate that the lattices of $(Ca_{2.95}Ba_{0.50}Sr_{0.50})(PO_4)_2O$ host combined from an expanded Ba-O/Sr-O and contracted Ca-O bonds which create different environments around the sites of Eu^{2+} ions doped in the lattice of $(Ca_{2.95}Ba_{0.50}Sr_{0.50})(PO_4)_2O$ phosphor and cause for the blue shifts and spectral broadening of Eu^{2+} activated $(Ca_{2.95}$ $Ba_{0.50}$ $Sr_{0.50})(PO_4)_2O$ phosphors.

Fig. 7 shows the emission spectra of $Ca_{4-x}(PO_4)_2O:xEu^{2+}$ with different Eu^{2+} concentration. It can be seen from the Fig., the optimal Eu^{2+} content was about $x = 0.10$. When the content of Eu^{2+} ions was over $x = 0.05$, concentration quenching occurred and emission intensity decreased with increasing Eu^{2+} ions concentration. Moreover, emission wavelength as well as emission intensity of the $Ca_{4-x}(PO_4)_2O:xEu^{2+}$ phosphors were changed by varying the concentration of Eu^{2+} ions. As the concentration of Eu^{2+} ions in the

45

host lattice was increased, the emission wavelength shifted slightly to a shorter wavelength. With an increase of the Eu^{2+} concentration x, the integrated emission intensity slightly increases with a breaking point $x \approx 0.10$, which establish its higher emission efficiency.

Upon excitation at a wavelength of 450 nm, the external quantum efficiency of $(Ca_{2.95}$ $Ba_{0.50}$ $Sr_{0.50})$ $(PO_4)_2$ $O:0.05Eu^{2+}$ and $(Sr,Ba)_2SiO_4:Eu^{2+}$ well known yellow phosphor are determined to be 38.7% and 70.9%, respectively. The lower quantum efficiencies of $(Ca_{2.95}$ $Ba_{0.50}Sr_{0.50})(PO_4)_2O:0.05Eu^{2+}$could be further enhanced by process optimization.

3.2. Application to White LEDs.

Figure 8 shows photometric and colorimetric quantities of the white LEDs under the following applied currents: 20, 50, 100, 150,

200, 250, 300 and 350mA. When the applied current was 350mA, the white LED have CIE color coordinate of (0.3354, 0.3448) at a white light (Tc = 5500 K) and an excellent *Ra* of 86.The CIE color coordinates shifted towards the white light region along the Planckian locus, the value of Ra decreased from 91.6 to 86.0 and the luminous efficiency decreased from 21.5 to 16.5 lm/W as the applied current was increased. In comparison with the blue InGaN chip pumped with YAG:Ce^{3+} phosphor (Ra = 75, CCT=7756K), and $LaSr_2AlO_5$ phosphor (R_a = 85-85, CCT = 4200-5500 K) (Deng et al., 2013; Huang *et al*., 2008), the white LEDs in this study shows higher Ra value and lower CCT value. Therefore, the (Ca, Ba, Sr)$_4(PO_4)_2O:Eu^{2+}$ phosphors are promising for application in excellent R_a white LEDs.
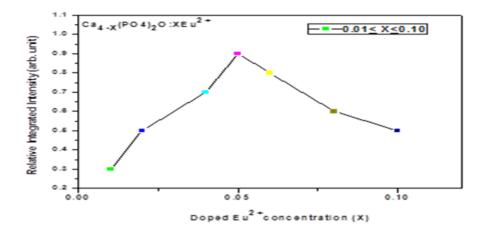
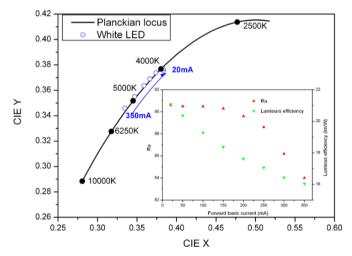**Figure 7**: The emission spectra of $Ca_{4-x}(PO_4)_2O:xEu^{2+}$ with different Eu^{2+} concentration

Figure 8: CIE chromatic coordinates, R_a and luminous efficiency (the inset) of the white LED using $(Ca_{2.95}Ba_{0.50}Sr_{0.50})(PO_4)_2O:0.05Eu^{2+}$ under various applied currents. The Planckian locus line and the points corresponding to color temperatures are indicate

4. Conclusions

In summary, a tunable red-to-yellow- emitting $Ca_{3.95-y-z}Ba_ySr_z)$ $(PO_4)_2O:0.05Eu^{2+}$ phosphors have been reported. The excitation spectrum shows broad band in the near-ultraviolet, ultraviolet and blue region, which matches well with blue chips $(Ca, Ba, Sr)_4$

47

$(PO_4)_2O:Eu^{2+}$ which is excitable over a broad range from 500 to 800nm when its emission can be adjusted from reg to yellow by changing Ba^{2+}/Sr^{2+} doping concentration. By applying $(Ca_{2.95}Ba_{0.50}Sr_{0.50})$ $(PO_4)_2$ $O:0.05$ Eu^{2+} phosphor on blue chip, we obtained a white LED device with high R_a of 86 and CCT value of 5450 K. Therefore, with the interesting tunable emission property, $(Ca, Ba)_4(PO_4)_2O: Eu^{2+}$ phosphor has great application potential as a good color conversion material for solid state lighting.

Acknowledgment

References

Bachmann, V., Ronda, C., and Meijerink, A., (2009). Temperature Quenching of Yellow Ce^{3+} Luminescence in YAG:Ce, *Chem. Mater.*, 21, 2077.

Deressa, G., Park, K.W., Jeong, H.S., Lim, S.G., Kim, H.J., Jeong, Y.S., and Kim, J.S., (2015). Spectral broadening of blue $(Sr, Ba)_5$ $(PO4)_3Cl$: Eu^{2+} phosphors by changing Ba^{2+}/Sr^{2+} composition ratio for high color rendering index, *J. Lumin*. **161**, 347.

Dorenbos, P., (2013). A review on how lanthanide impurity levels change with chemistry and structure of inorganic compounds, ECS*: J. Solid State Sci. Technol.***2**, R3001.

Huang, Y., Ding, Jang., KE, H., Cho, H., Lee, M., Jayasimhadri, S. Y., (2008). Luminescence properties of triple phosphate Ca_8 $MgGd$ $(PO_4)_7$: Eu^{2+} for white light-emitting diodes, J. Phys. D:Appl. Phys., 41, 095110.

48

Im, W., Brinkley, S., Hu, J. Mikhailovsky, A., Seshadri, S., DenBaars, R., (2010). $Sr_{2.975-x}Ba_xCe_{0.025}AlO_4F$: Highly Efficient Green-Emitting Oxy fluoride Phosphor for Solid State White Lighting, Chem. *Mater.*, **22**, 2842.

Kottaisamy, M., Jagannathan, R., Jeyagopal, P., Rao, R., Narayanan, R., (1994). Eu^{2+} luminescence in $M_5(PO_4)_3X$ apatites, where M is Ca^{2+}, Sr^{2+} and Ba^{2+}, and X is F^-, Cl^-, Br^- and OH, *J. Phy. D: Appl. Phys.***27**, 2210.

Ronda, C.R., (2008). Luminescence from Theory to Applications, VCH, Weinheim.

Schubert, E. F., and Kim, J. K., (2005). Solid- State Light source Getting Smart, *Scienc*e, **308**, 1274.

Setlur, A., Radkov, V. E., Henderson, S. C., J., Her, M. A., Srivastava, N. K., Kishore, M. Kumar, N., Aesram, D., Deshpande, A., Kolodin, A., Grigorov, L., Happek, U., (2010). Energy-efficient, high-color-rendering LED lamps using oxyfluoride and fluoride phosphors, *Chem. Mater.*, **22**, 4076.

Sommerdijk,. J. L., A. Bril, and A. W. de Jager, (1974).Two photon luminescence with ultraviolet excitation of trivalent praseodymium, *J. Lumin*., **8**, 341.

Wegh, R. T., Donker, H., Oskam, K. D., Meijerink, A., (1999). Visible quantum cutting in LiGdF4: Eu3+ through down conversion, *Science*, **288**, 663.

Wu, Y. D., Wang, T., Chen, C., Lee, K., Chen, H. K., (2011).A Novel Tunable Green- to Yellow-Emitting β-YFS: Ce^{3+} Phosphor for Solid-State Lighting, *ACS Appl. Mater. Interfaces*, **3**, 3195.

Yang, P., Yao, G.-Q., Lin, J.-H., (2004). Photoluminescence properties and energy level locations of RE^{3+} (RE = Pr, Sm, Tb, Tb/Ce) in CaAlSiN₃phosphors*, Inorg. Chem. Commun*. **7**, 302.

Zhou, L. H., Liang, P. A., Tanner, S., Zhang, D., Hou, C., Tao,Y., Huang, Y., Li, L., (2013). Luminescence, Cathodoluminescence and Ce^{3+}, Eu^{2+} energy transfer and emission enhancement

49

in the Sr_5 $(PO_4)_3$ $Cl:Ce^{3+},Eu^{2+}$ phosphor, *J. Mater. Chem. C*, **1**, 7155.

Zhou, X., Yang, X. Wang, Y., Zhao, X. Li, L., Li, Q., (2014).Luminescence and energy transfer in single-phased emission- tunable tri-color emitting phosphors of SrB_6O_{10}: Eu, Mn, *Alloy. Comp.*, **608**, 25.